Available online at www.sciencedirect.com
SCIENCE DIRECT
Chemical Physics Letters 422 (2006) 165–169
CHEMICAL PHYSICS LETTERS
www.elsevier.com/locate/cplett

Growth of MgO nanowires assisted by the annealing treatment of Au-coated substrates

Hyoun Woo Kim *, Seung Hyun Shim

School of Materials Science and Engineering, 253 Yong Hyun Dong, Nam Gu, Inha University, Incheon 402-751, Republic of Korea

Received 7 January 2006; in final form 14 February 2006
Available online 10 March 2006

Abstract

We synthesized crystalline MgO nanowires on Au-coated substrates by the heating of MgB_2 powders. We carried out the thermal annealing on Au-coated substrates prior to the MgO deposition process, affecting the morphology of the final MgO structures. The produced nanowires were of cubic MgO structures with diameters in the range of 40–200 nm. We discussed the possible growth mechanism. Photoluminescence spectrum of the MgO nanowires under excitation at 325 nm showed a visible light emission.

1. Introduction

Since the discovery of carbon nanotubes (CNTs), much technological and scientific excitement has been raised by the discovery of various forms of nanostructures [1–4]. Among them, one-dimensional (1D) structures including nanowires, nanobelts and nanowires are supposed to have potential applications to nanoelectronics and optoelectronics, owing to their novel physical properties. Magnesium oxide (MgO) is a typical wide-band-gap insulator, having found many applications as catalysis, additives in refractory, paint and superconductor products, and as substrates for thin film growth [5,6]. Accordingly, many research groups have reported on the synthesis of 1D MgO nanostructures [7–13], however, they generally studied from the viewpoint of the preparation method and characterization.

The CNT growth is known to depend strongly on the characteristics of metal catalyst, although the complete mechanism has not been determined. Therefore, we need to investigate the effect of the substrate material on the growth behavior of MgO nanostructures.

In the present communication, we applied thermal annealing treatment to the Au-coated substrates before we grow the MgO structures by a thermal evaporation of MgB_2 powders. Obtaining the MgO nanowires by controlling the predeposition annealing temperature, we have investigated the structural and photoluminescence (PL) properties of the as-prepared MgO nanowires.

2. Experimental

We employed Au-coated Si substrates. In order to fabricate the Au-coated Si substrates, we used Si as the starting material onto which a Au layer of about 3 nm thick was deposited by ion sputtering (Emitech, K757X). Since our objective was to investigate the effect of Au-coated substrate with respect to its morphology, we have preformed the thermal annealing treatment prior to MgO deposition, in which temperatures were in the range of 300–700 °C for 0.5 h in a flow of nitrogen (N_2) gas (flow rate; 500 standard cm^3/min).

The synthesis process was carried out in a quartz tube. The pure MgB_2 powders and the substrates, respectively, were placed on the lower and the upper holder in the center of the quartz tube inserted into a horizontal furnace. The vertical distance between the powders and the substrate with the Au-coated side downwards, was approximately 10 mm. During the experiment, the furnace was maintained at a temperature of 900 °C with the ambient gas ($Ar + O_2$) being at a constant total pressure of 2 Torr. The typical

* Corresponding author. Fax: +82 32 862 5546.
E-mail address: hwkim@inha.ac.kr (H.W. Kim).

0009-2614/$ - see front matter © 2006 Elsevier B.V. All rights reserved.
doi:10.1016/j.cplett.2006.02.062

percentage of O_2 and Ar partial pressure, respectively, were set to approximately 3 and 97%. After 2 h of evaporation, the furnace was allowed to cool down to room temperature.

The crystal structure of the products were examined by means of X-ray diffraction (XRD, X'pert MRD-Philips) analysis with Cu $K\alpha_1$ radiation ($\lambda = 0.154056$ nm) and incidence angle of 0.5°. The overview of the sample morphology was checked by scanning electron microscopy (SEM, Hitachi S-4200). Transmission electron microscopy (TEM) was performed by a filed emission electron microscope (Philips CM-200). For the TEM observation, the products were ultrasonically dispersed in acetone, and a drop of the solution was placed on a Cu grid coated with a porous carbon film. PL measurements were carried out by using a He–Cd laser line (325 nm, 55 mW) as the excitation source at room temperature.

3. Results and discussion

Fig. 1a–c shows the SEM images of the Au (3 nm-thick)-coated substrates prior to MgO deposition with the annealing temperature of 300, 500, and 700 °C, respectively. From the SEM images of the sample with the predeposition annealing at a temperature of 700 °C, we observe the relatively wide island-like structures, while we observe the relatively narrow particle-like structures in the pre-annealed samples in the range of 300–500 °C. We reveal that not only the width of Au structures but also the distance between the neighbouring structures in case of 700 °C-annealed sample is larger than those in case of 300–500 °C-annealed samples. The neighbouring Au particle-like structures generated by the predeposition annealing at 300–500 °C are not even completely disconnected. These results are consistent with our previous experiments, in which the Au film on Si(100) surfaces agglomerated and formed the cluster-like Au structures after annealing at a sufficiently high temperature of 600–700 °C [14]. Fig. 1c reveals that the lateral width of island-like structures is in the range of 40–500 nm.

Fig. 2a indicates the XRD spectrum of the final product without a predepostion annealing and Fig. 2b–d indicates the XRD spectra of the final products with the predeposition annealing at 300, 500, and 700 °C, respectively. Miller

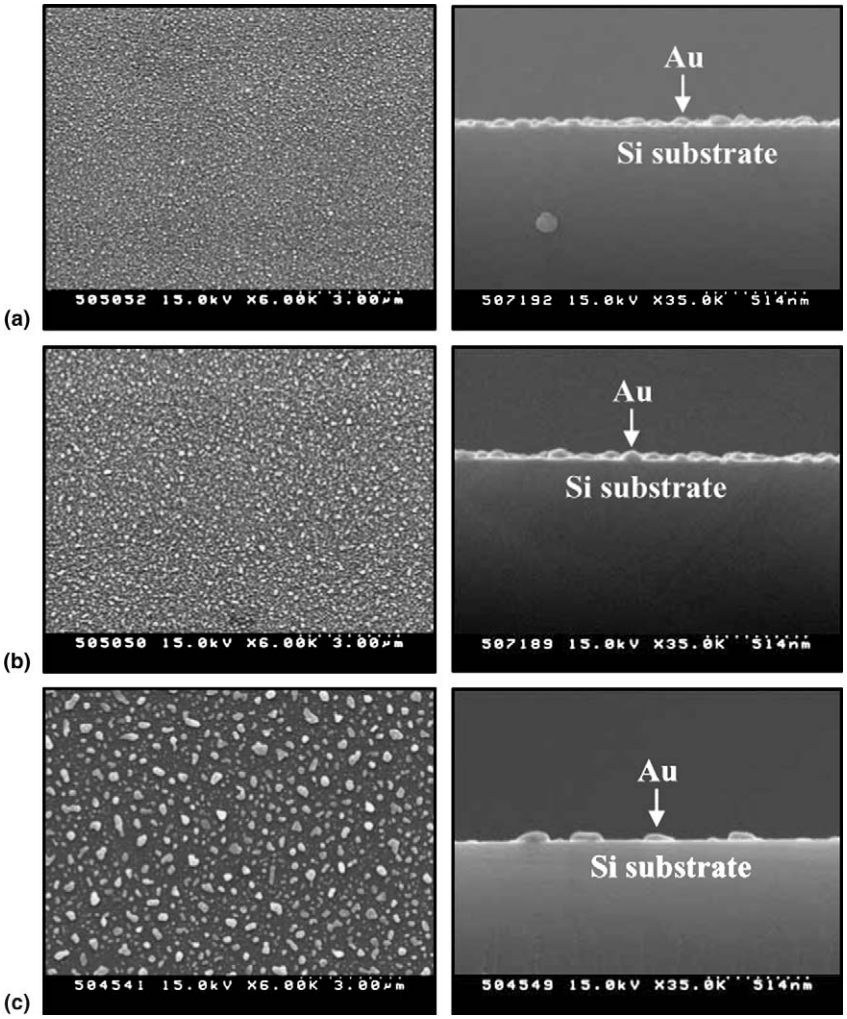

Fig. 1. Top-view and side-view SEM images of the Au (3-nm thick)-coated substrates with the predeposition annealing at: (a) 300, (b) 500, and (c) 700 °C.

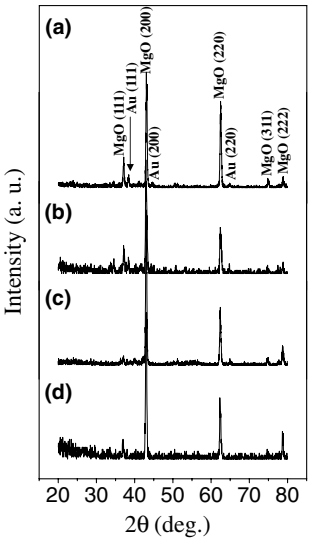

Fig. 2. XRD patterns recorded from the products: (a) without the predeposition annealing and with the predeposition annealing at (b) 300, (c) 500, and (d) 700 °C.

indices are indicated on each diffraction peak. The diffraction peaks of (111), (200), (220), (311), and (222) correspond to the cubic MgO structure with a lattice constant of $a = 0.421$ nm (JCPDS: 04-0829). Additionally, (111), (200), and (220) diffraction peaks of Au from the substrate were detected. XRD analysis reveal that products are MgO phase whether the predeposition annealing was performed or not and regardless of annealing temperature in the range of 300–700 °C.

Fig. 3a shows a typical SEM image of the final product without a predepostion annealing and Fig. 3b–d shows the typical SEM images of the final products with the predeposition annealing at 300, 500, and 700 °C, respectively. The product without predeposition annealing corresponds to the MgO films. The product with the predeposition annealing at 300 °C comprises the film-like structures, with the rock-shaped structures on the surface. The SEM image of the product with the predeposition annealing at 500 °C shows the rod-like structures on top of the MgO film, with the diameters in the range of 200–350 nm. The product with the predeposition annealing at 700 °C consists of relatively thin 1D structures. The top-view SEM image shown in Fig. 3e reveals that their diameters are in the range of 40–200 nm. Fig. 3f shows the enlarged SEM image of the product with the predeposition annealing at 700 °C, indicating that no catalyst particle can be seen at the tips of the 1D structures.

There are two well-accepted mechanisms for the growth of 1D nanostructures, viz. the vapor–liquid–solid (VLS)

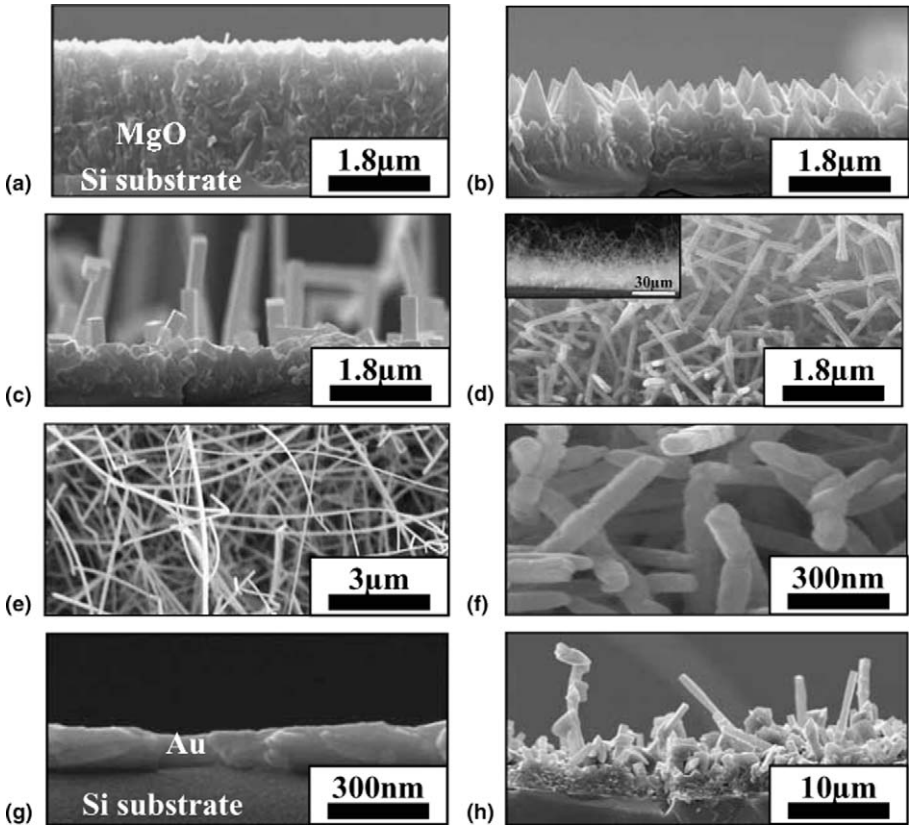

Fig. 3. Side-view SEM images of the product: (a) without the predeposition annealing and with the predeposition annealing at: (b) 300, (c) 500, and (d) 700 °C (upper left inset: low magnification SEM image). (e) Top-view and (f) high magnification SEM image of the product with the predeposition annealing at 700 °C. (g) Side-view SEM image of the Au-coated substrate with the Au thickness of 120 nm with the predeposition annealing at 700 °C. (h) Side-view SEM image of the product with the predeposition annealing at 700 °C with the 120-nm thick Au layer.

and the vapor–solid (VS) mechanisms. The VLS mechanism is a catalyst-assisted process, in which the metal catalyst particles act as a liquid-forming agent. In the present work, although Au-coated substrates were employed, the SEM and TEM analyses provided no evidence that the catalyst was present at the tips of the 1D structures. Hence, the growth mechanism of MgO nanostructures cannot be ascribed to the tip-growth VLS mechanism. Instead, there may be two possibilities. One is that this type of growth might be attributed to the VS mechanism, corresponding to a diffusion-limited process in a supersaturated environment. We surmise that Au is not easy to oxidize; thus, the elemental Au provides less additional oxygen to the growing MgO nanostructures, contributing to the production of thin 1D nanomaterials. On the contrary, a large oxygen supersaturation may activate secondary growth sites and heterogeneous nucleation on the side of the 1D structures, tending to produce wider or thicker structures in the VS mechanism. The other possibility may lie in the base-growth VLS mechanism. In this type of VLS process, the Au nanoparticle may stay at the bottom of the nanowires during the growth process. Similarly, previous work on the production of CNTs [15] revealed that the growth can be ascribed to the base growth mechanism, in which the metal catalyst remains situated at the bottom of the nanostructures.

Our previous experiments indicated that only film-like or thicker 1D structures were obtained by using the thicker Au layer, whether the predeposition annealing was performed or not. Fig. 3g shows the side-view SEM image of Au (120-nm thick)-coated substrate after the thermal annealing at 700 °C. Fig. 3h shows the SEM image of the associated final product, consisting of film-like structures and thick 1D structures. Although we have employed the predeposition annealing at 700 °C, the thin MgO nanowires was not obtained, presumably because 120-nm thick Au layer could not be transformed into the small enough Au islands. Therefore, we suppose that Au island provides the site for the independent growth of the 1D structure, while the wide Au layer substrate with many nucleation sites promote the agglomeration of thin 1D structures, producing the thick 1D structures or film-like structures. Also, as shown in Fig. 3b, c, we did not obtain the thin 1D structures by employing the predeposition annealing at 300–500 °C, presumably because the Au film was not transformed to the island-like structures with a wide interspace but to the smaller particle-like structures which are not completely disconnected. Since the width of Au island-like structures and the

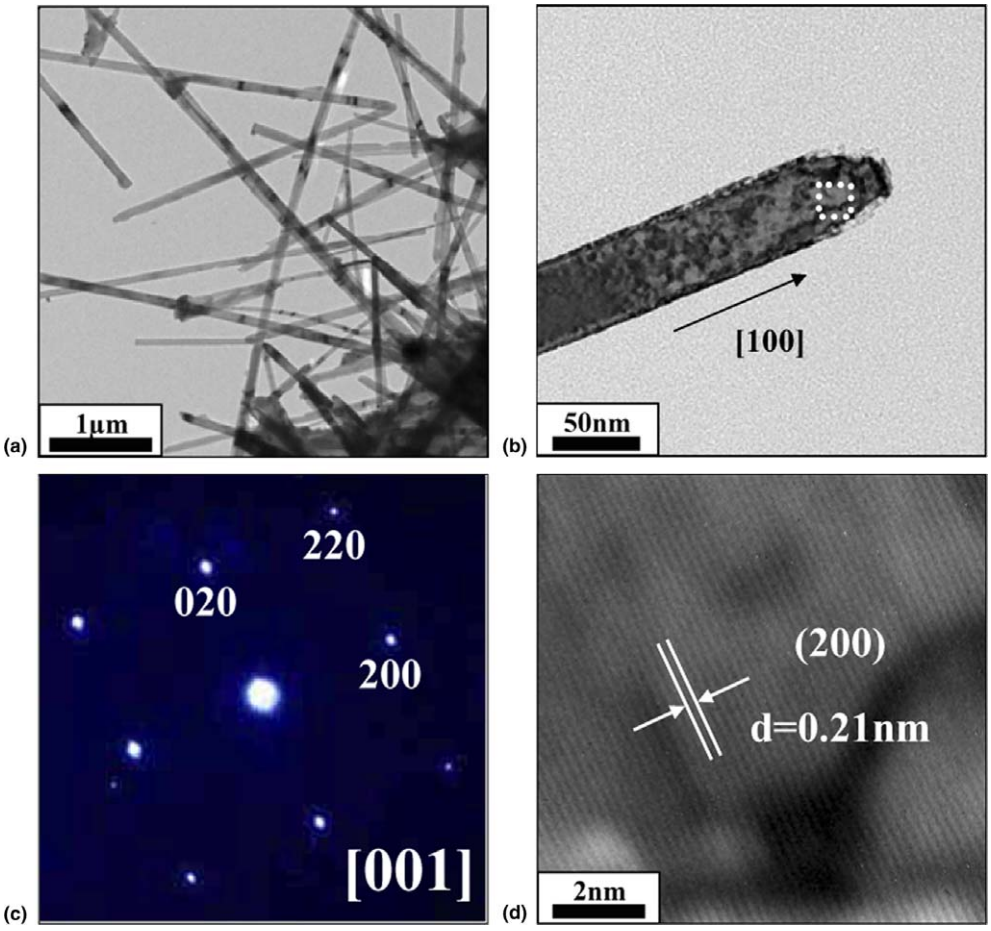

Fig. 4. (a) Low magnification TEM image of the product with the predeposition annealing at 700 °C. (b) TEM image of a single MgO nanowire. (c) Corresponding SAED pattern recorded along the [0 0 1] zone axis. (d) HRTEM image taken at the area marked with the dotted box in Fig. 4b.

diameters of MgO nanowires are of the similar value in the sample with a predeposition temperature of 700 °C, we surmise that both the growth location and diameter of MgO nanowires are controlled by the position and size of Au catalysts. Accordingly, we suggest that the growth of MgO nanowire is mainly controlled by the base-growth VLS mechanism. Meanwhile, as shown in Fig. 4b, the MgO nanowire had a non-uniform diameter along the growth direction, possibly indicating that the nanowire growth can also be controlled by the VS mechanism. Similarly, the growth of CdS nanobelts with a non-uniform width was controlled by both VS and tip-growth VLS mechanism [16,17]. Further systematic study is necessary.

For obtaining more detailed information about the obtained individual nanowires, we have carried out the TEM analysis. Fig. 4a is the low magnification TEM image of the product with the predeposition annealing at 700 °C. No spherical droplet or nanoparticle can be seen at tips of the nanowires. Fig. 4b exhibits the TEM image of a single nanowire with the width of approximately 50 nm. Fig. 4c shows an associated selected area electron diffraction (SAED) pattern. The SAED pattern, recorded perpendicular to the nanowire long axis, can be indexed for [0 0 1] zone axis of crystalline MgO. The length direction is supposed to be along the [1 0 0] direction, as shown in Fig. 4b,d is a high resolution TEM (HRTEM) image enlarging an area enclosed by the square in Fig. 4b, revealing a good crystallinity. The interplanar spacings are about 0.21 nm, corresponding to the (2 0 0) plane of cubic MgO.

The PL spectrum of the MgO nanowires at room temperature is shown in Fig. 5. There is an apparent broad emission band, which can be a superimposition of several peaks. After multi-peak Gaussian fitting to two major bands in Fig. 5, we found that the Gaussian curves fit the original curves almost perfectly. Therefore, the PL spectrum mainly consists of two bands, which peaks at approximately 438 and 507 nm, respectively. The similar blue emission with a peak position around 440–443 nm have been observed in the PL spectrum from MgO nanostructures fabricated by the carbon-related process [18,19]. Also, the similar blue-green band centered at 508 nm was observed from MgO nanobelts which was prepared by the simple evaporation of Mg powders [20]. Both blue and blue-green light emissions may originate from the defects in MgO, such as oxygen vacancy [21], Mg vacancies and interstitials, which induce the formation of new energy levels in the band gap of MgO. In the present study, high temperature evaporation may generate various structural defects, contributing to the observed visible emission.

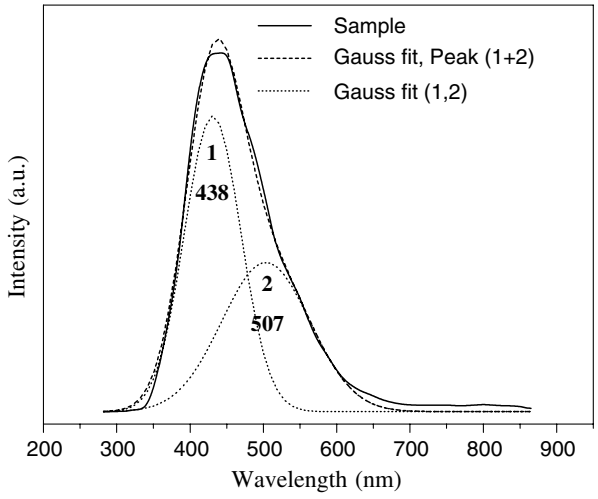

Fig. 5. Room-temperature PL spectrum of MgO nanowires with an excitation wavelength at 325 nm.

4. Conclusion

We have successfully fabricated MgO nanowires via a thermal evaporation method of heating MgB_2 powders. SEM images reveal that the formation of Au islands on substrates, by carrying out the predeposition annealing on Au-coated Si substrate, plays a crucial role in subsequently growing the MgO nanowires. XRD, HRTEM and SAED analyses coincidentally indicate that the nanowire is crystalline. The PL measurement with the Gaussian fitting shows apparent visible light emission bands centered at 438 nm and 507 nm.

Acknowledgement

This work was supported by Inha University Research Grant.

References

[1] S. Iijima, Nature 354 (1991) 56.
[2] C.B. Murray, C.R. Kagan, M.G. Bawendi, Science 270 (1995) 1335.
[3] J. Hu, T.W. Odom, C.M. Lieber, Acc. Chem. Res. 32 (1999) 435.
[4] Z.W. Pan, Z.R. Dai, Z.L. Wang, Science 291 (2001) 1947.
[5] R.Z. Ma, Y. Bando, Chem. Phys. Lett. 370 (2003) 770.
[6] Y.Q. Zhu, W.K. Hsu, W.Z. Zhou, M. Terrones, H.W. Kroto, D.R.M. Walton, Chem. Phys. Lett. 347 (2001) 237.
[7] P.D. Yang, C.M. Lieber, Science 273 (1996) 1836.
[8] Y.Q. Zhu, W.K. Hsu, W.Z. Zhou, M. Terrones, H.W. Kroto, D.R.M. Walton, Chem. Phys. Lett. 347 (2001) 337.
[9] Y. Li, Y. Bando, T. Sato, Chem. Phys. Lett. 359 (2002) 141.
[10] Y. Yin, G. Zhang, Y. Xia, Adv. Funct. Mater. 12 (2002) 293.
[11] J. Zhang, L. Zhang, X. Peng, X. Wang, Appl. Phys. A 73 (2001) 773.
[12] K.L. Klug, V.P. Dravid, Appl. Phys. Lett. 81 (2002) 1687.
[13] P. Yang, C.M. Lieber, J. Mater. Res. 12 (1997) 2981.
[14] K.C. Lee, N.H. Kim, B.-H. O, H.W. Kim, Mater. Sci. Forum 475–479 (2005) 3923.
[15] S. Fan, M.G. Chapline, N.R. Franklin, T.W. Tombler, A.M. Cassell, H. Dai, Science 283 (1999) 512.
[16] L.F. Dong, J. Jiao, M. Coulter, L. Love, Chem. Phys. Lett. 376 (2003) 653.
[17] L.F. Dong, J. Jiao, Microsc. Microanal. 11 (2005) 116.
[18] F.L. Deepak, P. Saldanha, S.R.C. Vivekchand, A. Govindaraj, Chem. Phys. Lett. 417 (2006) 535.
[19] K.P. Kalyanikutty, F.L. Deepak, C. Edem, A. Govindaraj, C.N.R. Rao, Mater. Res. Bull. 40 (2005) 831.
[20] J. Zhang, L. Zhang, Chem. Phys. Lett. 363 (2002) 293.
[21] G.H. Rosenblatt, M.W. Rowe, G.P. Williams Jr., R.T. Williams, Y. Chen, Phys. Rev. B 39 (1989) 10309.